2012-11

The role of insulin-like growth factors signaling in merlin-deficient human schwannomas

Ammoun, Sylwia

10.1002/glia.22391
Glia
Wiley

GLIA

GLIA 60:1721–1733 (2012)

The Role of Insulin-Like Growth Factors Signaling in Merlin-Deficient Human Schwannomas

SYLWIA AMMOUN, M. CAROLINE SCHMID, NATALIA RISTIC, LU ZHOU, DAVID HILTON, EMANUELA ERCOLANO, CAMILLE CARROLL, AND C. OLIVER HANEMANN*

Clinical Neurobiology, Peninsula Medical School, Plymouth University, Plymouth PL68BU, United Kingdom

KEY WORDS

human schwannoma; insulin-like growth factors; proliferation/adhesion/survival

ABSTRACT

Loss of the tumor suppressor merlin causes development of the tumors of the nervous system, such as schwannomas, meningiomas, and ependymomas occurring spontaneously or as part of a hereditary disease Neurofibromatosis Type 2 (NF2). Current therapies, (radio) surgery, are not always effective. Therefore, there is a need for drug treatments for these tumors. Schwannomas are the most frequent of merlin-deficient tumors and are hallmark for NF2. Using our *in vitro* human schwannoma model, we demonstrated that merlin-deficiency leads to increased proliferation, cell–matrix adhesion, and survival. Increased proliferation due to strong activation of extracellular-signal-regulated kinase 1/2 (ERK1/2) is caused by overexpression/activation of platelet-derived growth factor receptor-β (PDGFR-β) and ErbB2/3 which we successfully blocked with AZD6244, sorafenib, or lapatinib. Schwannoma basal proliferation is, however, only partly dependent on PDGFR-β and is completely independent of ErbB2/3. Moreover, the mechanisms underlying pathological cell–matrix adhesion and survival of schwannoma cells are still not fully understood. Here, we demonstrate that insulin-like growth factor-I receptor (IGF-IR) is strongly overexpressed and activated in human primary schwannoma cells. IGF-I and -II are overexpressed and released from schwannoma cells. We show that ERK1/2 is relevant for IGF-I-mediated increase in proliferation and cell–matrix adhesion, c-Jun N-terminal kinases for increased proliferation and AKT for survival. We demonstrate new mechanisms involved in increased basal proliferation, cell–matrix adhesion, and survival of schwannoma cells. We identified therapeutic targets IGF-IR and downstream PI3K for treatment of schwannoma and other merlin-deficient tumors and show usefulness of small molecule inhibitors in our model. PI3K is relevant for both IGF-IR and previously described PDGFR-β signaling in schwannoma.

INTRODUCTION

Deficiency of the tumor suppressor merlin causes spontaneous schwannomas, meningiomas, and ependymomas, which are also a feature of a hereditary disease neurofibromatosis Type 2 (NF2). Merlin belongs to Ezrin–Radixin–Moesin protein family (Rouleau et al., 1993) and regulates growth factor receptor signaling (Ammoun and Hanemann, 2011; McClatchey and Fehon, 2009). Schwannomas are the hallmark of NF2 and the most frequent of the merlin-deficient tumors for which we aim to define new therapeutic targets. Using our *in vitro* human schwannoma model (Rosenbaum et al., 1998), we have previously shown overexpression/activation of ErbB2/ErbB3 (Ammoun et al., 2010a) and platelet-derived growth factor receptor (PDGFR) (Ammoun et al., 2008) in human primary schwannoma cells and tissues resulting in increased activity of extracellular-signal-regulated kinase (ERK1/2) and AKT and enhanced proliferation (Ammoun et al., 2008, 2010a,b). PDGFR-β is important in schwannoma proliferation (Ammoun et al., 2008, 2010a) but not cell–matrix adhesion (Ammoun et al., 2008), an important characteristic of schwannoma (Flaiz et al., 2009a; Utermark et al., 2003b). Moreover, increased basal (nonstimulated) proliferation of schwannoma cells is only partly dependent on PDGFR-β (Ammoun et al., 2008) and is not responsive to ErbB2/ErbB3 inhibitors (Ammoun et al., 2010a), suggesting the involvement of additional factors. Ras is strongly activated in schwannoma involved only in basal (nonstimulated) ERK1/2 signaling independently on PDGFR (Ammoun et al., 2008). Lallemand et al. (2009) found that membrane accumulation of receptor tyrosine kinases is regulated by merlin. In addition to platelet-derived growth factors (PDGFs), insulin-like growth factors I/II (IGF-I/II) are relevant in rodent Schwann cells (Meier et al., 1999). IGF-I stimulates myelination in Schwann cells via the PI3K/AKT pathway (Ogata et al., 2004), control cell–matrix adhesion, proliferation, and survival (Meier et al., 1999; Schumacher et al., 1993) via ERK1/2 (Duan, 2003), AKT, focal adhesion kinase (FAK), and c-Jun N-terminal kinases (JNK) (Walsh et al., 2002) which are all strongly activated in schwannoma (Ammoun et al., 2008; Kaempchen et al., 2003). We therefore investigated the role of the IGF/IGF-IR system in proliferation, cell–matrix adhesion, and survival of human primary schwannoma cells. We show overexpression and activation of IGF-IR and overexpression and

Additional Supporting Information may be found in the online version of this article.

Grant sponsor: Children Tumour FoundationNorthcott Devon Medical FoundationAction Medical Research.

*Correspondence to: C. Oliver Hanemann, Clinical Neurobiology, Peninsula Medical School, The John Bull Building, Tamar Science Park, Research Way, Plymouth PL68BU, United Kingdom. E-mail: oliver.hanemann@pms.ac.uk

Received 30 April 2012; Revised 20 June 2012; Accepted 22 June 2012

DOI 10.1002/glia.22391

Published online 20 July 2012 in Wiley Online Library (wileyonlinelibrary.com).

release of IGF-I and IGF-II from schwannoma cells. IGF-IR triggers ERK1/2, AKT, JNK, and FAK phosphorylation/activation in schwannoma cells. We analyzed signaling pathways and showed that ERK1/2 is relevant for IGF-I-mediated increase in proliferation and adhesion, JNK for increased proliferation and AKT for survival. We suggest that, in addition to PDGFR (Ammoun et al., 2008, 2010a) and ErbB2/ErbB3 (Ammoun et al., 2010a), the IGF-system is important for schwannoma pathobiology. This is a novel observation broadening our knowledge about the pathobiology of schwannoma and other merlin-deficient tumors. Importantly, our findings have a future therapeutic relevance as using a small molecule PPP and monoclonal antibody R1507, we successfully inhibited IGF-R-mediated proliferation of human primary schwannoma cells. We also identified PI3K as a common target for IGF-IR and PDGFR, which when inhibited would block signaling mediated by both receptors.

MATERIALS AND METHODS

Culture of Human Primary Schwann and Schwannoma Cells

Human primary Schwann and schwannoma cells were isolated as described in our previous work (Rosenbaum et al., 1998). The study was approved by our Institutional Review Board. Schwann cells were isolated from peripheral nerves obtained from multiorgan donors not carrying any neurological disease after informed consent. Schwannomas were kindly provided by NF2 patients after informed consent. Diagnosis of NF2 was based on clinical criteria defined by the NIH Consensus Conference on Neurofibromatosis. Human malignant mesothelioma cell lines; merlin-deficient mesothelioma cell line (TRA) and merlin-expressing mesothelioma (HIB) were used as controls (Utermark et al., 2003a). Cells were cultured in complete medium (Growth Factor Medium): DMEM, 10% FCS, 0.5 μM forskolin, 10 nM β heregulin, 0.5 mM 3-isobutyl-1-methylxanthine, and 2.5 μg/mL insulin. For each experiment, samples from three-six different patients were used. Merlin expression was detected by western blotting using antimerlin antibody (Santa Cruz Biotechnology, Santa Cruz, CA). For every assay, tumors from three different patients were used. No discrepancies in the results between patients were observed. For proliferation assay, all the cells from different tumors were in early passages (1–2) as older passages displayed slower growth rate.

Inhibitors and Chemicals

GF109203X was from Tocris Bioscience (Bristol, UK). SU6656, FTI-277, and PPP were from Calbiochem (La Jolla, CA). R1507 was from Roche (Basel, Switzerland). SP600125 was from Affiniti, Wortmannin from Tocris, BEZ-235 from Novartis (Horsham, UK), short hairpin RNA (shRNA) FAK and IGF-IR from Open Biosystems (Huntsville, AL). DAPI and propidium iodide were from Sigma (St. Louis, MO) and MEK1/2 inhibitor U0126 (Du et al., 2010) from Promega (Madison, WI). Anti-FLAG tag antibodies were from Sigma and adenovirus expressing FLAG-tagged JNK-binding domain (JBD) of JNK-interacting protein-1 (JIP-1) (Harding et al., 2001) was a gift from Dr, Parkinson (Parkinson et al., 2004). IPA3 ("inhibitor targeting PAK1 activation" 2,2′-dihydroxy-1.1′-dinaphthylsulfide) (20 μM) (Flaiz et al., 2009b) and the control PIR-3.5 ("PAK1 inhibitor relative 3.5" 2-naphthalenol-6,6′-dithiobis) (20 μM) (Flaiz et al., 2009a,b) were gifts from J. Peterson, Philadelphia. Human recombinant-IGF-I was from Cell Sciences (Canton, MA) and Sigma and -IGF-II from Sigma. IGF-I and −II were used at a concentration of 100 ng/mL (Fiedler et al., 2006; Zhang et al., 2009). Most of these drugs have been previously tested in our human primary schwannoma model (Ammoun et al., 2008, 2010a; Flaiz et al., 2009b). PNGase F was from New England Biolabs (Herts, UK), and removal of carbohydrate residues was performed according to manufacturer instructions. For western blotting and proliferation assays all inhibitors were used at concentrations within their specificity and working concentration range which have been previously confirmed by others (Bennett et al., 2001; Du et al., 2010; Georgakis et al., 2006; Rexhepaj et al., 2010; Sakai et al., 2010; Toullec et al., 1991). FTI277 was used at higher concentration (30 μM) which inhibits all Ras subfamilies as confirmed by the manufacturer and other scientific articles (Kim et al., 2010; Lerner et al., 1995) and have been previously shown by us to inhibit Ras and basal but not PDGFR-mediated activity of ERK1/2 in schwannoma (Ammoun et al., 2008). U0126, SU6656, and wortmannin have been previously validated for human primary schwannoma cells (Ammoun et al., 2008, 2011, 2012). Concentration titration was done for SP600125 (data not shown), and R1507 as their starting concentrations were not effective. For survival assays, U0126 and SP600125 were used at much higher concentrations than their IC_{50}, however without any effect. FAK and IGF-IR, shRNA, was used in addition to chemical inhibitors. For JNK inhibition, adenovirus expressing FLAG-tagged JBD of JIP-1 was used in addition to the chemical inhibitor. For PI3K and IGF-IR, two different inhibitors were used for data confirmation.

shRNA Knockdown

GIPZ-shRNAmir lentiviral particles encoding a shRNA with nonsilencing sequence (mock) or sequences targeting specific genes, including human FAK (V2LHS_57326) and human IGF-IR (ready to use GIPZ viral particles, V2LHS_131070) were used. (1) Cells were seeded into 6-well plate to reach 70% confluence (Day 1); (2) cells were infected with 2.5μl virus per well in the full growth media containing 8 μg/mL protamine sulfate (Day 2); (3) growth media were replaced, 4 μg/mL puromycin was added into media for 48 h (Day 3). The knock down efficiency of each clone against nonsilencing control was verified by western blotting.

Reintroduction of Merlin

Mock (control adenovirus containing a GFP) and merlin wild type (recombinant adenovirus AdNF2) were gift from J. Testa (Xiao et al., 2005). Cells were infected for 24 h followed incubation with fresh GFM for additional 24 h.

Immunoblotting

Electrophoresis/western blotting (Kaempchen et al., 2003) were performed using antiphospho-IGF-I receptor Tyr1158/1162/1163 (Abcam, Cambridge, MA), antiactive-MAPK (anti-pThr$^{(183)}$-pTyr $^{(185)}$-ERK1/2) (Promega), antiphospho-AKT (Ser473) (Cell Signaling, Danvers, MA), antiphospho-FAK (Tyr925) (Cell Signaling), antiphospho-FAK (Tyr397) (Chemicon International, Temecula, CA), antiphospho-FAK (Tyr861) (Stressgen, New York, NY), antiphospho-JNK (Thr183/Tyr185) (Cell Signaling), anti-human-IGF-I (Abcam) and anti-human-IGF-II (Abcam and R&D Systems, Minneapolis, MN), anti-human-IGF-I-receptorβ (Cell Signaling), anti-human-IGF-II-receptor (R&D Systems), anti-FAK (Milipore, Watford, UK), and HRP-conjugated secondary antibodies (Biorad, Hercules, CA). ECL-plus (Amersham, Buckinghamshire, UK) was used for detection. Anti-Src (Cell Signaling), anti-AKT (Santa Cruz Biotechnology), anti-JNK1/2, and anti-ERK1/2 (Cell Signaling) were used to monitor total protein amount. Because short-term stimulations (10 min) do not affect protein expression levels (Lee et al., 2007), we have used a generic loading control Rho-GDI previously established for our system and which expression is not deregulated in schwannoma cells (Anti-RhoGDI antibody; Santa Cruz Biotechnology) (Hanemann et al., 2006). Actin or tubulin are not appropriate loading controls as schwannoma cytoskeleton is deregulated (Flaiz et al., 2009a,b). In some experiments, total protein was used for loading control which correlated with RhoGDI. In one experiment, GAPDH (Milipore) was used as a loading control. Images were scanned and processed using Corel Paint Shop Pro Photo XI software. Images represent the original data. The membranes were stripped after each probing, blocked and reprobed with new antibody. The stripping effectiveness was determined by using secondary antibody and developing.

Immunohistochemistry

Following 30 min blocking of endogenous peroxidase with 3% hydrogen peroxide, 4μm paraffin sections of formalin-fixed schwannoma tissues were pretreated with citrate buffer (pH 6) in a microwave for 30 min (Hanemann et al., 1997; Korinthenberg et al., 1997). Sections were counterstained with hematoxylin. Parallel section where stained with hematoxylin and eosin and showed no evidence of necrosis. Antibodies were applied overnight: antiphospho-IGF-I receptor Tyr1158/1162/1163 (Abcam), IGF-I (Abcam), and IGF-II (Abcam). Detection was performed with the Vectastain Universal Elite ABC kit (Vector Laboratories, Peterborough, UK). Controls were by omission of the primary antibody. Some sections were incubated with λ phosphatase (8,00,000 U/mL, at 30°C for 2 h New England Biolabs, Hitchin, UK).

TABLE 1. Primer Sequences for IGF Precursors

Primer name	Sequence (5′–3′)	Product size (bp)
IA Fw	AGGTGAAGATGCACACCATG	430
IA Rev	CTGCACTCCCTCTACTTGC	
IIA Fw	CTACAGTGAAGATGCACACC	380
IIA Rev	CTGCACTCCCTCTACTTGC	
IB Fw	GTATGGCTCCAGCAGTCG	240
IB Rev	GGATGTGTCTTTGGCCAAC	
IC Fw	GTATGGCTCCAGCAGTCG	222
IC Rev	CCTTCTCTGAGACTTCGTG	

Immunocytochemistry

The cells were fixed, permeabilized, and blocked as described (Flaiz et al., 2009a,b; Kaempchen et al., 2003). Localization of IGF-I was performed using anti-human-IGF-I (Abcam). Alexa Fluor 488-labeled phalloidin was used to visualize actin filaments (1:100; Molecular Probes, Eugene, OR). Multitrack imaging was performed using a Zeiss Confocal LSM510. Blocking peptide (BP) was used to demonstrate staining specificity.

Blocking of Primary Antibodies

0.4 μg/mL anti-human-IGF-I and -IGF-II antibodies were incubated with 5-fold excess of BP at 37°C for 2 h, then overnight at 4°C. Samples were centrifuged at 14,000 rpm/15 min/4°C. Supernatants were diluted in 1% BSA/TBS.

RNA Extraction and RT-PCR

Total RNA was extracted from schwannoma cells from 4 different patients using GenElute^{TM} Mammalian Total RNA Miniprep Kit (Sigma) and treated with DNA-*free*^{TM} Kit (Ambion, Huntingdon, UK) according to the manufacturers' instructions. Total RNA from muscle and liver were from Clontech (Saint-Germain-en-Laye, France). 0.5 μg of total RNA from each sample was reverse transcribed using the High Capacity cDNA Archive Kit (Ambion) according to manufacturer's instructions. Conditions for the PCR amplification of cDNA were: denaturation at 95°C 15 s, annealing at 55°C 60 s, and extension at 72°C 30 s for 40 cycles (Table 1).

Cell Growth and Viability

Cells were cultured as described (Ammoun et al., 2008) for 24 h under different conditions: DMEM, 100 ng/mL human recombinant-IGF-I, 100 ng/mL human recombinant-IGF-II or GFM. BrdUrd incorporation was per-

formed as described in Ammoun et al. (2006) using anti-BrdUrd antibody (Calbiochem) and ALEXA-Fluor488 labeled secondary antibody (Molecular Probes/Invitrogen, Paisley, UK). For JNK inhibition, schwannoma cells were preincubated in defined medium (Morgan et al., 1994) for 1 h before infection with GFP control or JBD-expressing adenovirus. After 24 h, medium was changed to DMEM, and cells were stimulated with IGF-I (100 ng/mL) for additional 24 h. Infection efficiency was determined by anti-FLAG tag primary (Sigma) and ALEXA-Fluor488 labeled secondary antibodies (Sigma). Inhibitors were added 40 min before stimulation. Total cell number was determined by DAPI (1 μg/mL) and cell viability by propidium iodide (2.5 μg/mL).

Adhesion Assay

Adhesion assay was performed as described in Utermark et al. (2003b). Cells were stimulated with 100 ng/mL human recombinant-IGF-I or IGF-II or with GFM. Inhibitors were added 40 min before stimulation.

Data Analysis

Student's two-tailed t tests and ANOVA were used. All experiments were repeated at least three times using at least three independent batches of cells from different individuals. ns (not significant): $P > 0.05$; *: $P < 0.05$; **: $P < 0.01$; ***: $P < 0.001$. In figures, mean ± SEM is given.

RESULTS

IGF-IR is Strongly Overexpressed, Glycosylated, and Activated in Schwannoma

Primary human schwannoma cells (NF2−/−) strongly overexpress IGF-IR compared with normal human Schwann cells (NF2+/+) (Fig. 1a) which is reversed by merlin reintroduction suggesting direct correlation between merlin and receptor expression (Fig. 1b). IGF-IR is strongly phosphorylated, in basal (nonstimulated) conditions, in schwannoma cells compared with normal Schwann cells (Fig. 1c) which is potentiated by recombinant 100 ng/mL IGF-I (Fig. 1d) and reversed by merlin reintroduction (Fig. 1e). Human schwannoma tissues (Fig. 1f first panel) also showed strong cytoplasmic and nuclear staining of phosphorylated IGF-IR compared with three normal nerve biopsies, which displayed only weak nuclear and almost no cytoplasmic staining (Fig. 1f third panel). Staining was performed on schwannomas from five different patients and showed fairly uniform cytoplasmic immunoreactivity throughout the tumors, but variable nuclear staining (Fig. 1f first panel and Supp. Info. Fig. 4a). Nuclear localization of IGF-IR correlates with receptor's tumorigenicity previously shown in other tumors (Sehat et al., 2010). Pretreatment of tissue with phosphatase decreased signal intensity (Fig. 1f middle picture). Additionally human merlin-deficient mesothelioma cells (TRA) express IGF-IR at ~10 times higher levels than merlin-expressing mesothelioma (HIB) cells (Fig. 1g) used as a control for merlin-mediated pathological changes. IGF-IR is glycosylated (Fig. 1h). No difference in glycosylation intensity between Schwann and schwannoma cells was observed (Fig. 1h). IGF-IIR is equally expressed in Schwann and schwannoma cells (Fig. 1i first panel) and reintroduction of merlin did not affect IGF-IIR expression (Fig. 1i second panel).

IGF-I and IGF-II are Strongly Overexpressed and Released in Schwannoma

IGF-I (Fig. 2a,c) and IGF-II (Fig. 2d) are strongly overexpressed in schwannoma cells (NF2−/−) detected by western blotting. Strong overexpression of IGF-I precursor was also observed (Fig. 2b,c) as for mature IGF-I. The presence of three IGF-I precursor isoforms IGF-I IA, −IIA, and −IC, but not −IB were detected by PCR in schwannoma cells (Supp. Info. Fig. 1). Only merlin-deficient human schwannoma (NF2−/−) and human merlin-deficient mesothelioma (TRA) (Fig. 2e,f,h) but not human merlin-expressing mesothelioma (HIB) cells overexpressed IGF-I or precursor isoforms. Cell lines were used to confirm the role of merlin-deficiency in the abnormalities investigated. IGF-II is overexpressed in human schwannoma cells (NF2−/−) (Fig. 2g,h). The expression of IGF-I precursor, mature IGF-I, and IGF-II are decreased on merlin reintroduction (Fig. 2i–k). Schwannoma cells released IGF-I and IGF–II into the media at higher levels than Schwann cells, detected by western blotting in cell culture media on 24 h starvation (Fig. 2l,m), suggesting a possibility for autocrine signaling. Specificity of IGF-I and IGF-II bands were examined using BPs (Fig. 2l,m bottom panels). As total protein levels detected by Ponsceau S directly correlated with the intensity of nonspecific general bands on IGF-I/II probing (Supp. Info. Fig. 2 and previous publications Ammoun et al., 2011), we normalized to the later. General bands were used as loading control for western blots on cell culture media as there is are no known loading markers in media. In Fig. 2l, m bottom panels recombinant IGF-I and IGF-II peptides alone were loaded on gels to monitor the specificity of BPs and correct molecular weight of proteins detected in culture media. Nuclear and cytoplasmic localization of IGF-I and IGF-II was observed in schwannoma tissues ($n = 5$; Fig. 2n bottom first and second panels) (Schedlich et al., 2003). Normal tissues expressed IGF-I and IGF-II weaker ($n = 4$; Fig. 2n upper first and second panels). Staining for IGF-I and IGF-II was fairly uniform throughout the tissues observed in tumors from five different patients, although there was some variation with nuclear immunoreactivity, and in the case of IGF-II, cytoplasmic intensity (Fig. 2n bottom first and second panels and Supp. Info. Fig. 4b,c). Immunocytochemistry demonstrates a specific IGF-I staining in the nucleus and cytoplasm in schwannoma cells (Fig. 2o first picture). BP was used to confirm staining specificity (Fig. 2o second picture).

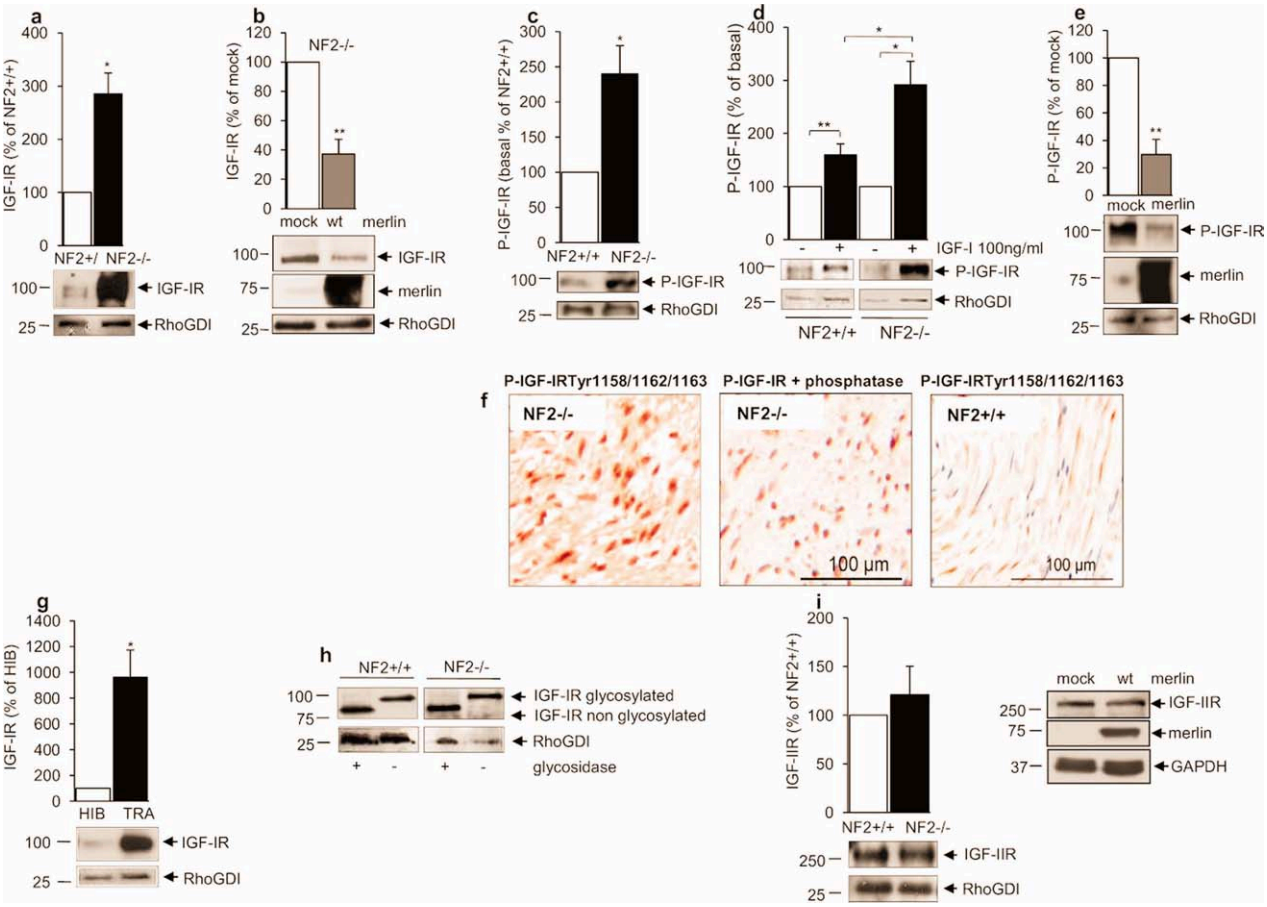

Fig. 1. IGF-I/II receptors' expression, activation, and glycosylation in merlin-positive/deficient cells. (a) IGF-IR is strongly overexpressed in schwannoma cells (NF2−/−) compared with Schwann cells (NF2+/+). (b) IGF-IR overexpression is reversed by the reintroduction of wild type merlin (wt, $n = 4$), but not the mock (control adenovirus containing a GFP). (**c**) Phosphorylated IGF-IR (P-IGF-IR) is strongly expressed in schwannoma cells (NF2−/−) in basal (nonstimulated) conditions ($n = 5$), (**f**) and in human schwannoma tissues ($n = 5$, first panel) compared with normal tissues (NF2+/+) ($n = 4$, third panel). (**d**) IGF-IR phosphorylation is increased on stimulation of schwannoma cells with recombinant IGF-I (100 ng/mL) compared with Schwann cells (NF2+/+), (**e**) which is reversed by reintroduction of merlin. (**g**) IGF-IR is overexpressed in merlin-deficient human mesothelioma (TRA, $n = 4$) but not merlin-positive human mesothelioma (HIB, $n = 4$). (**h**) IGF-IR is glycosylated in both schwannoma and Schwann cells. Cells were treated with or without glycosidase then checked with anti-IGF-IR antibody. (**i**) IGF-IIR is equally expressed in both schwannoma and Schwann cells ($n = 3$; first panel) independently on merlin expression (second panel). In (c), (d), and (e), the cells were starved for 24 h, in (c) cells were lysed directly and in (d) and (e) stimulated with IGF-I (100 ng/mL) for 5 min before lysing. In (a), (c), and (i), the data are normalized to NF2+/+. In (b), the data are normalized to the basal levels (nonstimulated) and in (g) to HIB. In (b) and (e), the data are normalized to mock adenovirus infected cells. Experiments in (d) were run independently on different gels therefore only the ratio basal versus IGF-I stimulated signal could be compared within the same cell type and different cell types. Basal activities between cell types could not be compared. RhoGDI served as a control and Western blotting were quantified. ns (not significant): $P > 0.05$; *: $P < 0.05$; **: $P < 0.01$; ***: $P < 0.001$. In figures, mean ± SEM is given. [Color figure can be viewed in the online issue, which is available at wileyonlinelibrary.com.]

Dissection of IGF-I-Mediated Signaling Pathways in Human Primary Schwannoma Cells

IGF-I stimulation of schwannoma cells leads to strong phosphorylation of FAK at Tyr925 and Src at Tyr416 and strongly activates ERK1/2, AKT, and JNK

Autophosphorylation of FAK at Tyr397 and Src-mediated phosphorylation at Tyr861 were not increased (Fig. 3a,c). IGF-I (100 ng/mL, 5 min) (Fiedler et al., 2006) strongly phosphorylated FAK at Src phosphorylation site Tyr925 (Fig. 3b; $n = 3$). Accordingly, Src was phosphorylated by IGF-I (100 ng/mL, 5 min) at Tyr416 (Fig. 3d; $n = 3$). IGF-I (100 ng/mL, 5 min) potentiated basal ERK1/2 (Fig. 3e), AKT (Fig. 3f; $n = 3$), and JNK (Fig. 3g; $n = 3$) activity in primary human schwannoma cells. Total levels of FAK, Src, ERK1/2, AKT, and JNK were unaffected (Fig. 3b,e,f, g; $n = 3$).

IGF-IR-mediated activation of ERK1/2 engages Src/FAK/Ras/PI3K/PKC, JNK Src/FAK/Ras/PI3K/PKC/PAK, and AKT Ras/PI3K/PAK pathways

To elucidate the signaling pathways involved in IGF-IR mediated activation of AKT, ERK1/2, and JNK in schwannoma cells (NF2−/−), we used shRNA for IGF-IR

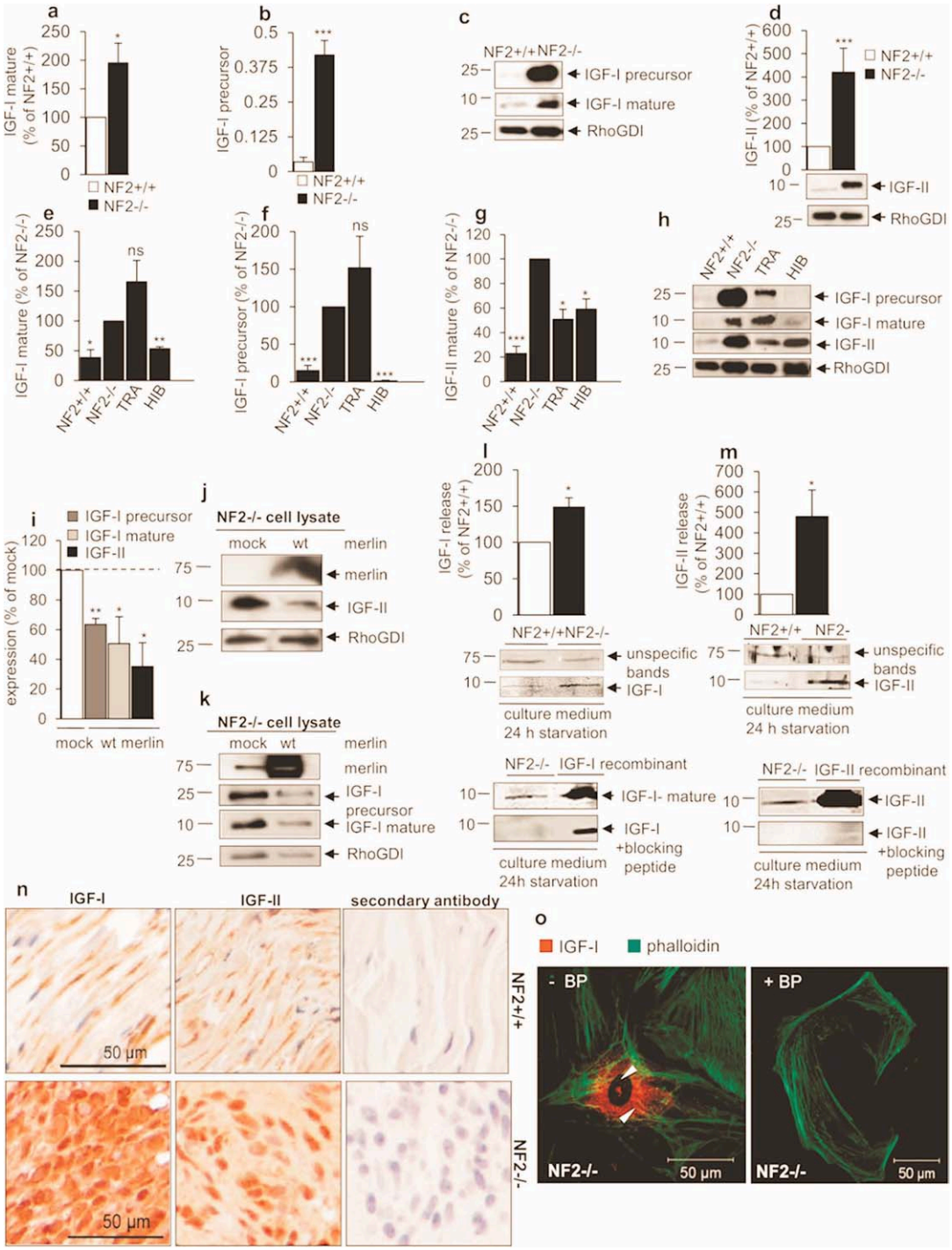

Fig. 2. Expression and release of IGF-I and IGF-II in human primary schwannoma cells. (a) IGF-I, (b) and (c) IGF-I precursors ($n = 7$) and (d) IGF-II ($n = 6$) are overexpressed in schwannoma cells (NF2−/−) compared with normal Schwann cells (NF2+/+, $n = 5$). (e, f, and h) Mature and precursor IGF-I are overexpressed in merlin-deficient schwannoma (NF2−/−, $n = 7$) and merlin-deficient mesothelioma (TRA, $n = 4$) cells compared with Schwann cells (NF2+/+, $n = 5$) and human merlin-positive mesothelioma (HIB, $n = 4$). (g and h) IGF-II is expressed strongest in merlin-deficient schwannoma (NF2−/−, $n = 6$) cells. (i–k) Reintroduction of wild type merlin (wt), but not mock control (GFP only) into schwannoma cells (NF2−/−) decreases intracellular expression of mature IGF-I (i and k, $n = 5$), IGF-I precursor (i and k, $n = 4$) and IGF-II (i and j, $n = 5$). Band in (k) mock is caused due to spill over of the lysates. (**l** and **m**) Increased release of IGF-I (l, $n = 5$) and IGF-II (m, $n = 3$) from schwannoma cells compared with Schwann cells ($n = 5$ for IGF-I and $n = 3$ for IGF-II). Specificity of antibodies is demonstrated in the bottom panels using blocking peptides. Cells were cultured in serum-free medium (DMEM) for 24 h, medium was collected and IGF-I/II detected by western blotting. Unspecific bands served as control. (**n**) shows that IGF-I and IGF-II are strongly expressed *in vivo* in schwannoma tissues (NF2−/−) ($n = 5$) compared with normal tissues (NF2+/+) shown by immunohistochemistry, scale bar = 50 µm ($n = 4$). (**o**) shows, by immunocytochemistry, a specific nuclear localization of IGF-I (left picture) which was abrogated with blocking peptide (BP) (right picture). In (a), (d), (l), and (m), the data are normalized to NF2+/+, in (e), (f), and (g) to NF2−/− and in (i) to mock adenovirus infected cells. ns (not significant): $P > 0.05$; *: $P < 0.05$; **: $P < 0.01$; ***: $P < 0.001$. In figures, mean ± SEM is given. [Color figure can be viewed in the online issue, which is available at wileyonlinelibrary.com.]

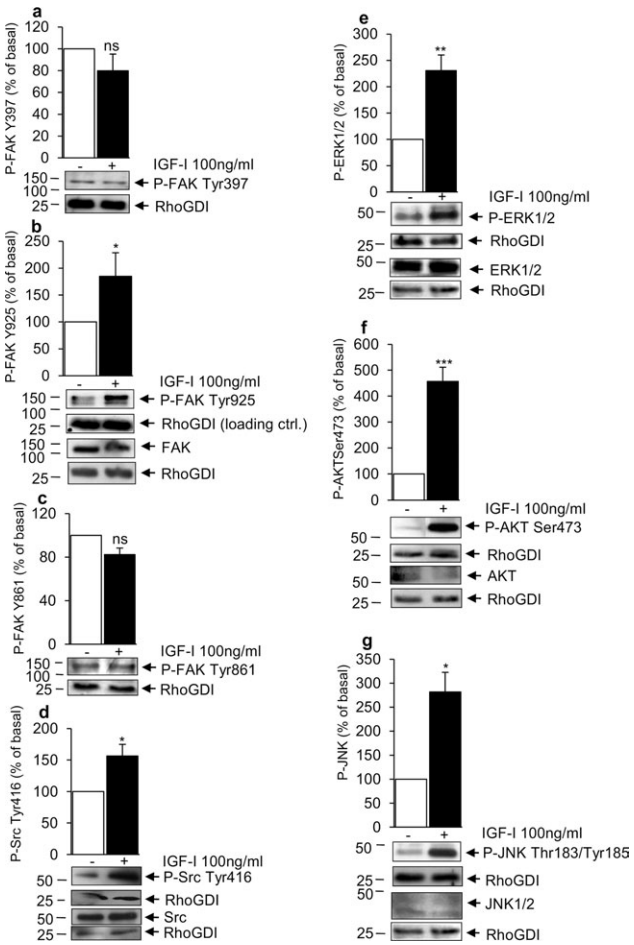

Fig. 3. Activation of IGF-I-mediated signaling pathways in human primary schwannoma cells. (a–c) IGF-I (100 ng/mL, 5 min) potentiates FAK phosphorylation at Tyr925 but not Tyr397 or Tyr861. (d–g) IGF-I (100 ng/mL, 5 min) stimulates Src, ERK1/2, AKT, and JNK phosphorylation ($n = 3$). In all experiments, data are normalized to basal (nonstimulated) and corrected to the loading control RhoGDI. Levels of total FAK, Src, ERK1/2, AKT, and JNK are not changed on short term (5 min) stimulation with 100 ng/mL IGF-I. ns (not significant): $P > 0.05$; *: $P < 0.05$; **: $P < 0.01$; ***: $P < 0.001$. In figures, mean ± SEM is given.

and FAK (Supp. Info. Fig. 3a,b) and various inhibitors previously established in our model and by others in the concentrations described (Ammoun et al., 2008; Du et al., 2010; Duggan et al., 2007; Flaiz et al., 2009b; Georgakis et al., 2006; Kim et al., 2010; Momcilovic et al., 2008; Rexhepaj et al., 2010; Sakai et al., 2010; Shi et al., 2001). Activity of AKT, ERK1/2, and JNK were investigated simultaneously on the same membrane for each experiment followed striping and reprobing of the membrane allowing us to additionally look at specificity in our model (Fig. 4d–x compare SU6656 (e, l, and s), shRNA FAK (f, m, and t), FTI (g, n, and u), wortmannin (h, o, and v), GF109203X (i, p, and w), and IPA3 (j, q, and x)).

AKT. Basal AKT activity was decreased by shRNA IGF-IR (Fig. 4a and Supp. Info. Fig. 3a) supporting autocrine signaling in schwannoma. Src inhibitor SU6656 (4 μM) (Sakai et al., 2010) and PKC inhibitor GF109203X (5 μM) (Duggan et al., 2007) (Fig. 4d,e,i), did not inhibit IGF-I (100 ng/mL)-stimulated AKT phosphorylation. Additionally, FAK knock down with shRNA (Supp. Info. 3b) did not decrease IGF-I-mediated AKT activity (Fig. 4d,f and Supp. Info. Fig. 3b). Ras inhibitor FTI 277 (30 μM) (Kim et al., 2010) and PI3K inhibitor wortmannin (1 μM) strongly inhibited AKT phosphorylation (Fig. 4d,g,h). PAK inhibitor IPA3 (20 μM), but not the structurally related control compound Pir3.5 (data not shown), significantly inhibited IGF-I-mediated AKT activation (Fig. 4d,j).

ERK1/2. Basal ERK1/2 activity is decreased by shRNA IGF-IR (Fig. 4b and Supp. Info. Fig. 3a) supporting autocrine signaling in schwannoma. SU6656 (4 μM) (Fig. 4k,l), shRNA for FAK (Fig. 4k,l and Supp. Info. Fig. 3b), FTI-277 (30 μM) (Fig. 4k,n), wortmannin (1 μM) (Fig. 4k,o) and GF109203X (5 μM) (Fig. 4k,p) (Toullec et al., 1991) strongly inhibited IGF-I-mediated ERK1/2 activation. IPA3 (20 μM), had no effect on IGF-I-mediated ERK activity (Fig. 4k,q).

JNK. Basal JNK activity was decreased by shRNA IGF-IR (Fig. 4c and Supp. Info. Fig. 3a) supporting autocrine signaling in schwannoma. SU6656 (4 μM) (Fig. 4r,s), FAK shRNA (Fig. 4r,t and Supp. Info. Fig. 3b), FTI 277 (30 μM) (Fig. 4r,u), wortmannin (1 μM) (Fig. 4r,v) and GF109203X (5 μM) (Fig. 4r,w) strongly inhibited IGF-IR-mediated JNK phosphorylation. IPA3 (20 μM), but not control compound Pir3.5 (data not shown), significantly inhibited IGF-IR mediated JNK activation (Fig. 4r,x).

IGF-IR-mediated AKT, ERK1/2, and JNK activation was inhibited by Ras inhibitor FTI (30 μM) used at the same concentration as in a previous article on PDGFR which inhibited Ras activity but not PDGFR-mediated signaling (Ammoun et al., 2008). In summary, IGF-IR-mediated activation of ERK1/2 and JNK engages Src/FAK/Ras/PI3K/PKC. AKT activation involved Ras/PI3K pathway but not Src/FAK (Wymann et al., 2003). PI3K acts as a convergence point for ERK1/2, AKT, and JNK cascades. PAK seems not involved in ERK1/2 activation but its inhibition decreases AKT and JNK activity after IGF-I stimulation (Fig. 7). An autocrine effect of IGF-I is observed as shRNA for IGF-IR decreases basal (nonstimulated with recombinant IGF-I) activity of AKT, ERK1/2, and JNK, suggesting that autocrine levels of IGF-I keep the base line activity of those kinases constantly elevated.

In the studies dissecting the IGF-I-mediated signaling pathways in human primary schwannoma cells, tumors from three different patients were used. No discrepancies were observed when comparing the results from different patients.

IGFI-R Activation Increases Proliferation and Cell–Matrix Adhesion of Schwannoma Cells

Proliferation

In schwannoma cells, IGF-I (100 ng/mL) and IGF-II (100 ng/mL) increased the number of proliferating cells

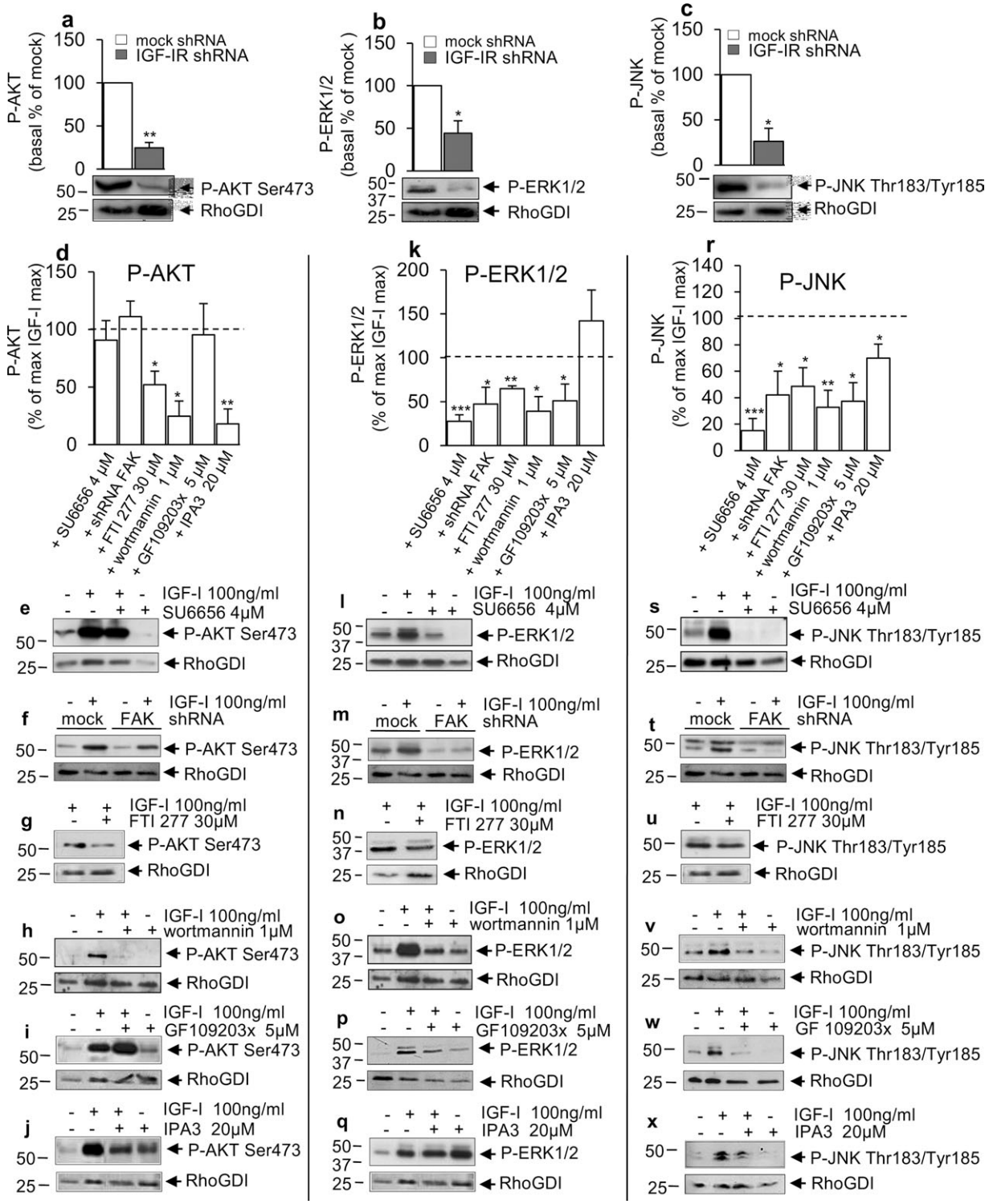

Fig. 4. Dissection of IGF-I-mediated signaling pathways in human primary schwannoma cells. AKT, ERK1/2, and JNK pathways were analyzed using shRNA IGF-IR, Src inhibitor SU6656, shRNA FAK, PI3K inhibitor wortmannin, Ras inhibitor FTI-277, PKC inhibitor GF109203X, and PAK inhibitor IPA3 at established concentrations. (a–c) shRNA IGF-IR decreases basal activity of AKT (n = 3), ERK1/2 (n = 3), and JNK (n = 3). (d–j) AKT pathway is dependent on Ras (n = 3), PI3K (n = 3), and PAK (n = 3), and independent of Src (n = 3), FAK (n = 3), and PKC (n = 3). (k–q) ERK1/2 and (r–x) JNK pathways involve Src (n = 3)/FAK (n = 3)/Ras (n = 3)/PI3K (n = 3)/PKC (n = 3). (k and q) ERK1/2 is independent, and (r and x) JNK dependent of PAK. Cells were starved for 24 h; SU6656, wortmannin and GF109203X were added 40 min before stimulation. IPA3 was added 10 min and FTI-277 24 h before stimulation. Dotted lines display noninhibited IGF-I response (100%). In (a)–(c), the data are normalized to basal mock shRNA and in (d), (k), and (r) to IGF-I max response (100%).

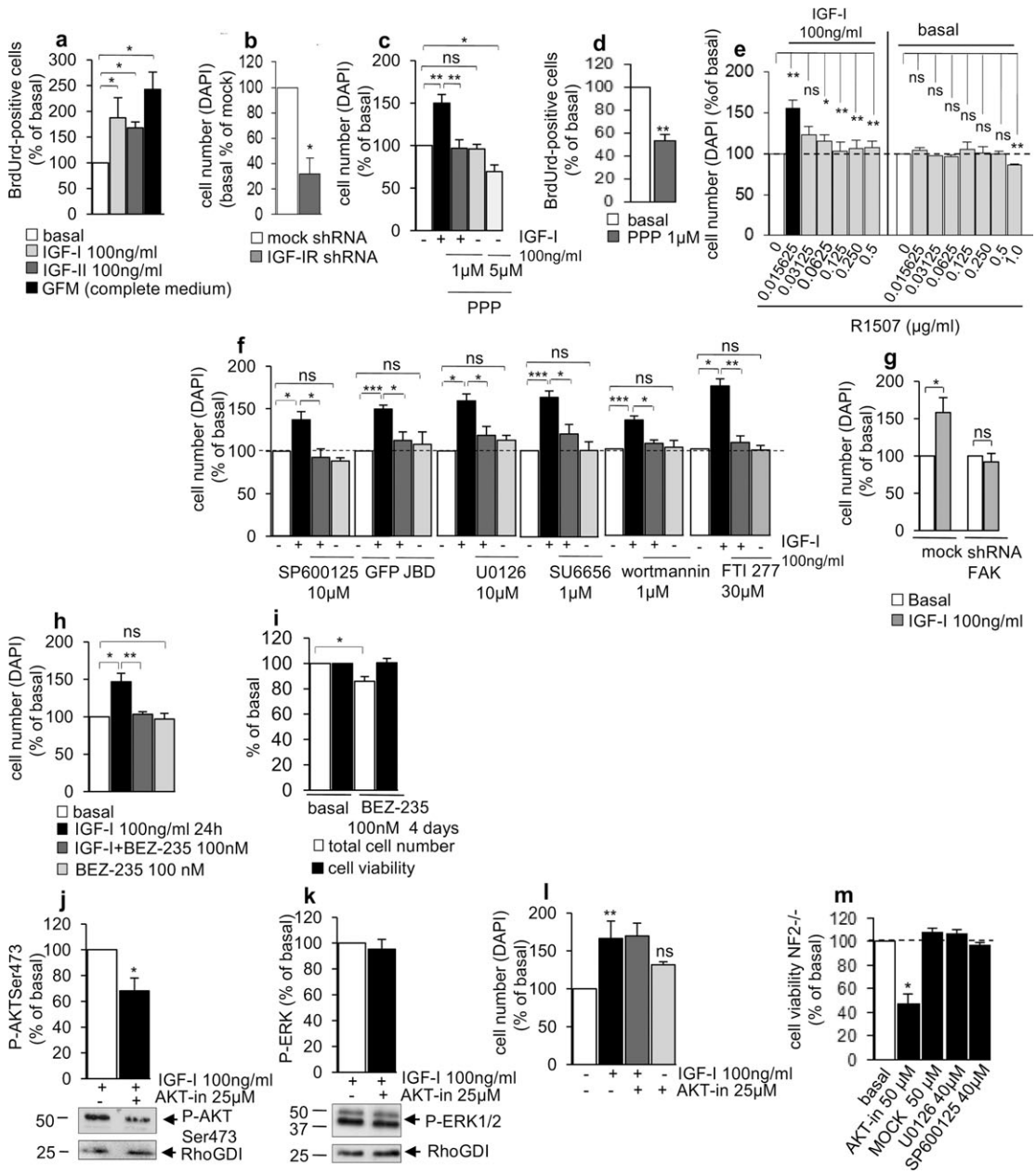

Fig. 5. IGF-IR-mediated proliferation, survival of human primary schwannoma cells. (**a**) Compared with basal, IGF-I and IGF-II stimulate schwannoma proliferation (BrdUrd) equally, but less than full growth medium (GFM). (**b–e**) Basal proliferation is decreased by shRNA IGF-IR ($n = 3$), IGF-IR inhibitor PPP (5 μM; BrduUrd method, $n = 3$) and (1 μM; DAPI method, $n = 3$), and monoclonal antibody R1507 (1 μM, $n = 3$). (b–e) IGF-I-mediated proliferation is inhibited by IGF-IR inhibitors PPP (1 μM) and R1507 (0.015625–0.5 μg/mL). (**f** and **g**) JNK inhibitor SP600125 ($n = 3$) or JBD of JIP-1($n = 3$), MEK1/2 inhibitor U0126 ($n = 3$), Src inhibitor SU6656 ($n = 3$), PI3K inhibitor wortmannin ($n = 3$), Ras inhibitor FTI-277 ($n = 3$), and shRNA for FAK ($n = 3$) inhibited IGF-IR-mediated proliferation. (**h**) A 24 h incubation with mTor/PI3K inhibitor BEZ-235 (100 nM, $n = 3$) inhibits IGF-I-mediated schwannoma proliferation. (**i**) A 4 days incubation of schwannoma cells with BEZ-235 (100 nM) decreases basal proliferation with no effect on cell viability. Cell culture medium was changed to serum-free DMEM medium and inhibitors were added 30 min before 24 h or 4 days incubation with/or without recombinant IGF-I 100 ng/mL. For expression of the JBD of JIP-1, schwannoma cells were infected with JBD-expressing adenovirus for 24 h. (**j**) AKT-in (25 μM, $n = 3$) inhibits phosphorylation of AKT, but not, (**k**) ERK1/2 ($n = 3$). (**l**) AKT is not involved in IGF-I mediated proliferation. Cells were treated with AKT-in (25 μM) for 12 h before incubation with IGF-I (100 ng/mL) for 24 h in serum-free DMEM medium. (**m**) AKT-in (50 μM, $n = 3$), but not the structurally related control compound "mock" inhibit schwannoma viability. MEK1/2 inhibitor U0126 (40 μM, $n = 3$) and JNK inhibitor SP600125 (40 μM, $n = 3$) do not affect schwannoma viability. ns (not significant): $P > 0.05$; *: $P < 0.05$; **: $P < 0.01$; ***: $P < 0.001$. In figures, mean ± SEM is given. In (e), white bars represent basal nonstimulated cells, black bars IGF-I stimulated cells without inhibitor, gray bars IGF-I stimulated cells treated with the inhibitor in left panel or nonstimulated cells treated with the inhibitor right panel. Proliferation at 0 μg/mL R1507 is without IGF stimulation, 0.015625 μg/mL is the first data point with stimulation. We have included unstimulated in most of our graphs as showing that growth factor stimulation works is an important control in each experiment.

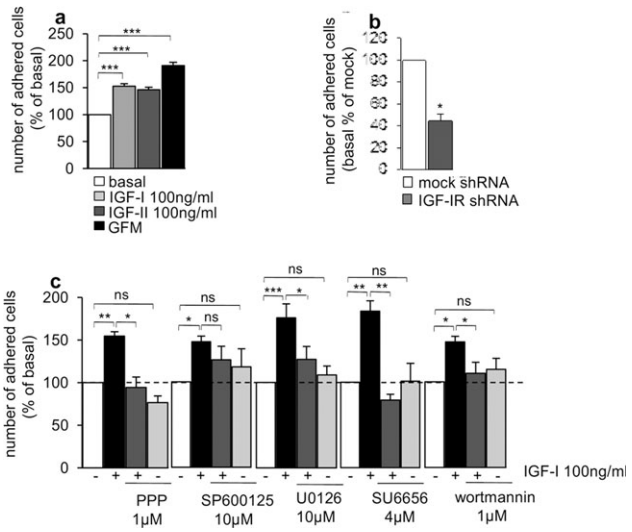

Fig. 6. IGF-IR-mediated cell matrix adhesion of human primary schwannoma cells. (a) IGF-I (100 ng/mL, $n = 9$) and IGF-II (100 ng/mL, $n = 3$) stimulate schwannoma cell–matrix adhesion equally, but less than full growth medium (GFM, $n = 8$). (b) Basal (nonstimulated) adhesion decreases on IGF-IR knock down with shRNA ($n = 3$). (c) IGF-I-mediated adhesion decreases on treatment with IGF-IR inhibitor PPP (1 μM, $n = 3$), JNK inhibitor SP600125 (10 μM, $n = 6$), MEK1/2 inhibitor U0126 (10 μM, $n = 3$), Src inhibitor SU6656 (4 μM, $n = 3$), and PI3K inhibitor wortmannin (1 μM, $n = 5$) indicating dependence on the ERK1/2 but not JNK pathway involving Src and PI3K. The cells were starved for 24 h, detached, preincubated with inhibitors for 30 min, stimulated with IGF-I (100 ng/mL), seeded again, and incubated for 3 h. In upper left and right panels, the data are normalized to the basal (nonstimulated) values. In bottom panel, the data are normalized basal mock shRNA. ns (not significant): $P > 0.05$; *: $P < 0.05$; **: $P < 0.01$; ***: $P < 0.001$. In figures, mean ± SEM is given.

(BrdUrd, Fig. 5a). As IGF-I and IGF-II act through the same receptor IGF-IR, we concentrated on IGF-I-mediated proliferation using inhibitors described above. In addition to DAPI, we used BrdUrd staining which is more sensitive method.

Basal proliferation (nonstimulated) of schwannoma cells was decreased by shRNA IGF-IR (Fig. 5b), 5 μM IGF-IR inhibitor PPP (Ohshima-Hosoyama et al., 2010) (Fig. 5c, DAPI), 1 μM PPP (Girnita et al., 2004) (Fig. 5d, BrdUrd), and by a monoclonal antibody against IGF-IR , currently in Phase I clinical trials, R1507 at 1 μg/mL (Fig. 5e right panel) (Gong et al., 2009; Kolb et al., 2010; Kurzrock et al., 2010). These data further support an autocrine loop in human primary schwannoma cells. IGF-I-stimulated (100ng/mL, Fig. 5e left panel) proliferation was decreased to the basal levels by IGF-IR inhibitors PPP (1 μM) and R1507 (0.125 μg/mL), lower concentrations (0.015625 μg/mL) was not effective and 0.03125 μg/mL decreased IGF-I-mediated proliferation only partially (Fig. 5c,e), MEK1/2 inhibitor U0126 (10 μM) (Fig. 5f third panel) and JNK inhibitor SP600125 (10 μM) (Bennett et al., 2001) (Fig. 5f first panel) suggesting ERK1/2 and JNK for being mitogenic for schwannoma on IGF-IR stimulation. JBD-GFP a negative regulator of JNK was also effective in the inhibition of IGF-I-mediated proliferation (Fig. 5f second panel). shRNA FAK decreased IGF-I-mediated schwannoma proliferation (Fig. 5g). Because Src, Ras, and PI3K are involved in IGF-IR-mediated ERK1/2 and JNK activation, we tested whether inhibitors of any of those kinases inhibit IGF-I-mediated proliferation. Src inhibitor SU6656 (1 μM), Ras inhibitor FTI277 (30 μM) (Ammoun et al., 2008; Kim et al., 2010), and PI3K inhibitor wortmannin (1 μM) (Rexhepaj et al., 2010; Shi et al., 2001) inhibited IGF-I-mediated proliferation of schwannoma cells (Fig. 5f). As PI3K cross talks to ERK1/2, AKT, and JNK (Figs. 4 and 7), we tested also dual mTor/PI3K small molecular inhibitor BEZ-235 (100 nM) which inhibited IGF-IR-mediated schwannoma proliferation (24 h treatment) (Fig. 5h). Basal schwannoma proliferation was decreased after 4 days' treatment with BEZ-235 (100 nM) without affecting cell viability (Fig. 5i).

None of the inhibitors was toxic at concentrations used (data not shown), and Src inhibitor SU6656, Ras inhibitor FTI277, PI3K inhibitor wortmannin, and MEK1/2 inhibitor U0126 were already validated in schwannoma model (Ammoun et al., 2008, 2011). AKT inhibitor peptide (AKT-in) (25 μM) which inhibited AKT by ~40% (Fig. 5j) but not ERK (Fig. 5k) did not decrease IGF-I-mediated proliferation (Fig. 5l). Thus, IGF-I-mediated proliferation recruits JNK and ERK1/2 but not AKT (Figs. 5f and 7).

Cell survival

Three days treatment with 50 μM AKT-in decreased schwannoma cell viability compared with AKT-in mock (Fig. 5m) (Hiromura et al., 2004). Neither MEK1/2 inhibitor U0126 (40 μM) nor JNK inhibitor SP600125 (40 μM) (Momcilovic et al., 2008) affected schwannoma cells' viability (Fig. 5m), suggesting that AKT but not ERK1/2 or JNK is a prosurvival in schwannoma.

Adhesion

Both IGF-I (100 ng/mL, 3 h) and IGF-II (100 ng/mL, 3 h) induced cell–matrix adhesion in schwannoma cells (Fig. 6a). This was not pronounced as with GFM but reached up to 50% (Fig. 6a). shRNA IGF-IR decreased basal (nonstimulated) adhesion of schwannoma cells suggesting autocrine signaling (Fig. 6b).

IGF-IR inhibitor PPP (1 μM) and MEK1/2 inhibitor U0126 (10 μM) completely inhibited IGF-I-mediated adhesion whereas JNK inhibitor SP600125 (10 μM) had no effect (Fig. 6c second panel). Src inhibitor SU6656 (4 μM) and PI3K inhibitor wortmannin (1 μM) (Fig. 6c fourth and fifth panels) completely inhibited IGF-I-mediated adhesion of schwannoma cells.

In summary, this article demonstrates the overexpression and activation of IGF-IR in human schwannoma (Fig. 7). IGF-IR ligands IGF-I and IGF-II are also overexpressed and released (Fig. 7) leading to increased activation of FAK, Src, ERK1/2, JNK1/2, and AKT (Fig. 7). IGF-IR-mediated activation of ERK1/2 engages Src/FAK/Ras/PI3K/PKC, JNK Src/FAK/Ras/PI3K/PKC/PAK and AKT Ras/PI3K/PAK pathways (Fig. 7). ERK1/2 mediates IGF-IR stimulated proliferation and adhesion of schwan-

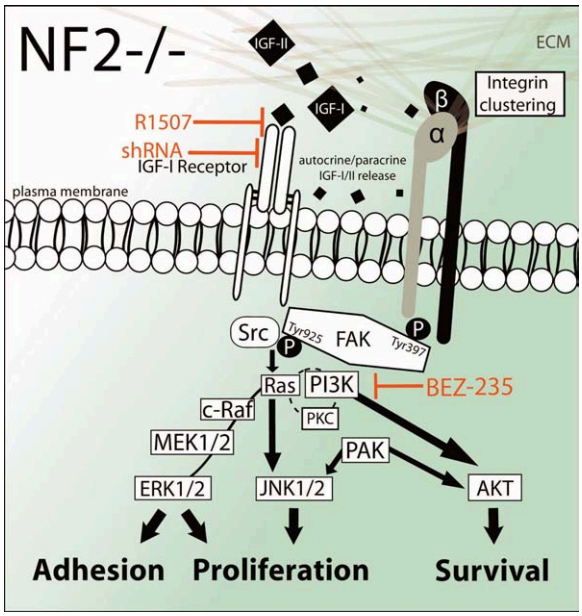

Fig. 7. Postulated IGF-IR-mediated signaling pathways in human primary schwannoma cells. In schwannoma, IGF-IR and integrins are overexpressed and activated. IGF-I and IGF-II are upregulated and released. Stimulated IGF-IR activates Src and Ras. Active Src phophorylates FAK, already autophosphorylated at Tyr397 via integrins, at the additional tyrosine site Tyr925 important for coupling active Ras to Raf/MEK1/2/ERK1/2 and MEKK1/MEKK4/7/JNK pathways. Ras, activated PI3K, C-Raf, and MEKK1 result in ERK1/2, AKT, and JNK activation. PAK contributes to JNK and AKT but not ERK1/2 activation. FAK couples to JNK and ERK1/2 but not AKT pathways. IGF-IR-stimulated ERK, JNK, and AKT share a common targetable kinase PI3K which is inhibited by mTor/PI3K inhibitor BEZ-235. ERK1/2 and JNK are responsible for increased growth, ERK1/2 for enhanced cell–matrix adhesion and AKT for survival of schwannoma cells. IGF-I-mediated schwannoma proliferation was successfully targeted by IGF-IR inhibitor R1507 (Phase I). [Color figure can be viewed in the online issue, which is available at wileyonlinelibrary.com.]

noma cells, JNK1/2 promotes adhesion and AKT survival (Fig. 7). IGF-IR-mediated pathological changes were normalized using a monoclonal antibody targeting IGF-IR R1507 and IGF-IR shRNA (Fig. 7). PI3K is a common kinase for IGF-IR mediated ERK1/2, JNK1/2, and AKT activation and can be successfully targeted by small molecule inhibitor BEZ-235 (Fig. 7).

DISCUSSION

We demonstrate strong overexpression of IGF-IR, and ligands IGF-I/IGF-II triggering activation of ERK1/2, JNK, and AKT pathways and show relevance for increased proliferation, adhesion, and survival of human primary schwannoma cells. We dissected downstream signaling cascades to identify potential therapeutic targets and test two small molecule inhibitors.

IGF-IR overexpression is in line with previously reported findings of membrane accumulation and overexpression of growth factor receptors in merlin-deficient cell lines (Lallemand et al., 2009). We show activation of IGF-IR in schwannoma cells and human schwannoma tissues compared with Schwann cells. Strong glycosylation increases IGF-IR attachment to the cell membrane resulting in decreased internalization and degradation (Carlberg and Larsson, 1996). Unexpectedly, IGF-IR glycosylation is equal in schwannoma and Schwann cells suggesting that IGF-IR activity in schwannoma cells must involve other mechanisms such as disruption of cell-to-cell contact allowing receptors to recycle to the cell surface which has shown to be inhibited by merlin (Flaiz et al., 2008; Lallemand et al., 2009; Li et al., 2010). IGF-IIR regarded as a tumor suppressor (Hebert, 2006) is equally expressed in schwannoma and Schwann cells. We show overexpression and release of IGF-I and IGF-II, relevant in Schwann cell biology, from schwannoma cells compared with Schwann cells suggesting that autocrine signaling is relevant in schwannoma development acting in concert with autocrine IGF-I and IGF-II. The autocrine circuit is demonstrated by the negative regulation of basal proliferation, adhesion, and signaling pathways by shRNA IGF-IR and further supported by proliferation assays with IGF-IR inhibitors PPP and R1507. Immunohistochemistry showed that IGF-IR, IGF-I, and IGF-II, in addition to the cytoplasm, localizes to the nucleus in schwannoma tissues which has been shown in other cells to promote tumor development (Schedlich et al., 2003; Sehat et al., 2010). To understand the targetability of IGF-IR signaling in schwannoma, we investigated different signaling pathways activated in schwannoma cells on IGF-IR stimulation. Despite replacing cell culture medium with fresh medium just before stimulation with exogenous IGF-I and IGF-II, we cannot exclude a small additional autocrine effect at least in the longer term experiments. However, we show clear stimulation of a variety of pathways due to IGFI/II. We show increased FAK phosphorylation at the Src phosphorylation site Tyr925 on cell stimulation with IGF-I (100 ng/mL, 5 min). Phosphorylation of FAK at its autophosphorylation site Tyr397, known to be triggered by β integrins (Zhao and Guan, 2009) strongly overexpressed in human schwannoma (Utermark et al., 2003b), is not potentiated further by IGF-I but likely is basally high which is necessary for further phosphorylation at Tyr925 (Zhao and Guan, 2009). The phosphorylation of FAK at Tyr925 is important for its coupling to Ras/Raf/MEK/ERK cascade upregulated in schwannoma (Ammoun et al., 2008). Indeed, we show that FAK shRNA blocked IGF-I-triggered ERK activation in schwannoma cells. Using various inhibitors established in our model (Ammoun et al., 2008, 2011), we show that ERK and JNK pathways involve Src/FAK/Ras/PI3K and PKC. AKT is activated via Ras/PI3K pathway (Fig. 7).

We demonstrate that IGF-I and IGF-II are mitogenic for schwannoma cells suggesting that, in addition to PDGF (Ammoun et al., 2008) and heregulin (Ammoun et al., 2010a), IGF-I and IGF-II are relevant in schwannoma. IGF-I-mediated increase in schwannoma proliferation engages JNK and ERK1/2 but not AKT which is prosurvival. This supports a previous demonstration of decreased viability of primary vestibular schwannoma cells when treated with phosphoinositide-dependent ki-

nase-1 inhibitor OSU-03012 (Lee et al., 2009). However, the inhibition of AKT decreases survival only partially suggesting that other prosurvival pathways may be active, making cells not addicted to AKT. The inhibition of AKT leads to decreased cell viability only when AKT-in are used at high concentrations for 3 days. Inhibition of AKT had no effect on schwannoma proliferation which could be due to a previously described positive feedback toward increased expression of IGF-IR and ErbB3 (Chandarlapaty et al., 2011). We also show that pathological schwannoma cell–matrix adhesion engaging IGF-I involves Src/PI3K/ERK1/2 pathway. In summary (Fig. 7), we suggest that IGF-IR mediates proliferation and adhesion involving different pathways, ERK1/2 and JNK for proliferation and ERK1/2 for adhesion. AKT regulates cell survival, previously shown to be enhanced in schwannoma cells (Utermark et al., 2005).

From this data and published data, it seems likely that inhibition of schwannoma growth would possibly require inhibition of several targets. Our results support two possible treatment options: (1) combinational therapy targeting IGF-IR and PDGFR; PDGFR inhibitors Sorafenib and Nilotinib (currently in Phase 0 clinical trials on NF2 patients) (Ammoun et al., 2008, 2011) and IGF-IR inhibitor R1507 (current data) have been already validated in schwannoma. (2) Therapy targeting a common molecule downstream of overactivated receptors. PI3K is such therapeutic target which has been previously shown to be involved in PDGFR-mediated ERK1/2 and AKT activation (Ammoun et al., 2008) and, as shown in this study, provides a common link for IGF-I-mediated ERK1/2, AKT and JNK pathways (Fig. 7). Here, we successfully used mTor/PI3K inhibitor BEZ-235 to significantly decrease basal and completely inhibit IGF-I-mediated schwannoma proliferation. As the inhibition of PI3K would inhibit all currently known pathways activated in schwannoma (Ammoun et al., 2008), the development of acquired resistance via compensation mechanisms would be negligible. As schwannomas are located outside of blood–brain barrier, drug delivery to the tumor should not be problematic. We suggest that results from using our human *in vitro* model for schwannoma will allow us to speed up bench to bed transition and reprofile drugs, directly in Phase 0 clinical trials.

ACKNOWLEDGMENT

R1507 was kindly provided by Roche and BEZ-235 by Novartis.

REFERENCES

Ammoun S, Cunliffe CH, Allen JC, Chiriboga L, Giancotti FG, Zagzag D, Hanemann CO, Karajannis MA. 2010a. ErbB/HER receptor activation and preclinical efficacy of lapatinib in vestibular schwannoma. Neuro Oncol 12:834–843.

Ammoun S, Flaiz C, Ristic N, Schuldt J, Hanemann CO. 2008. Dissecting and targeting the growth factor-dependent and growth factor-independent extracellular signal-regulated kinase pathway in human schwannoma. Cancer Res 68:5236–5245.

Ammoun S, Hanemann CO. 2011. Emerging therapeutic targets in schwannomas and other merlin-deficient tumors. Nat Rev Neurol 7:392–399.

Ammoun S, Lindholm D, Wootz H, Akerman KE, Kukkonen JP. 2006. G-protein-coupled OX1 orexin/hcrtr-1 hypocretin receptors induce caspase-dependent and -independent cell death through p38 mitogen-/stress-activated protein kinase. J Biol Chem 281:834–842.

Ammoun S, Ristic N, Matthies C, Hilton DA, Hanemann CO. 2010b. Targeting ERK1/2 activation and proliferation in human primary schwannoma cells with MEK1/2 inhibitor AZD6244. Neurobiol Dis 37:141–146.

Ammoun S, Schmid MC, Triner J, Manley P, Hanemann CO. 2011. Nilotinib alone or in combination with selumetinib is a drug candidate for neurofibromatosis type 2. Neuro Oncol 13:759–766.

Ammoun S, Schmid MC, Zhou L, Ristic N, Ercolano E, Hilton DA, Perks CM, Hanemann CO. 2012. Insulin-like growth factor-binding protein-1 (IGFBP-1) regulates human schwannoma proliferation, adhesion and survival. Oncogene 31:1710–1722.

Bennett BL, Sasaki DT, Murray BW, O'Leary EC, Sakata ST, Xu W, Leisten JC, Motiwala A, Pierce S, Satoh Y, Bhagwat SS, Manning AM, Anderson DW. 2001. SP600125, an anthrapyrazolone inhibitor of Jun N-terminal kinase. Proc Natl Acad Sci U S A 98:13681–13686.

Carlberg M, Larsson O. 1996. Stimulatory effect of PDGF on HMG-CoA reductase activity and N-linked glycosylation contributes to increased expression of IGF-1 receptors in human fibroblasts. Exp Cell Res 223:142–148.

Chandarlapaty S, Sawai A, Scaltriti M, Rodrik-Outmezguine V, Grbovic-Huezo O, Serra V, Majumder PK, Baselga J, Rosen N. 2011. AKT inhibition relieves feedback suppression of receptor tyrosine kinase expression and activity. Cancer Cell 19:58–71.

Du J, Sun C, Hu Z, Yang Y, Zhu Y, Zheng D, Gu L, Lu X. 2010. Lysophosphatidic acid induces MDA-MB-231 breast cancer cells migration through activation of PI3K/PAK1/ERK signaling. PLoS One 5:e15940.

Duan C. 2003. The chemotactic and mitogenic responses of vascular smooth muscle cells to insulin-like growth factor-I require the activation of ERK1/2. Mol Cell Endocrinol 206:75–83.

Duggan SV, Lindstrom T, Iglesias T, Bennett PR, Mann GE, Bartlett SR. 2007. Role of atypical protein kinase C isozymes and NF-kappaB in IL-1beta-induced expression of cyclooxygenase-2 in human myometrial smooth muscle cells. J Cell Physiol 210:637–643.

Fiedler J, Brill C, Blum WF, Brenner RE. 2006. IGF-I and IGF-II stimulate directed cell migration of bone-marrow-derived human mesenchymal progenitor cells. Biochem Biophys Res Commun 345:1177–1183.

Flaiz C, Ammoun S, Biebl A, Hanemann CO. 2009a. Altered adhesive structures and their relation to RhoGTPase activation in merlin-deficient Schwannoma. Brain Pathol 19:27–38.

Flaiz C, Chernoff J, Ammoun S, Peterson JR, Hanemann CO. 2009b. PAK kinase regulates Rac GTPase and is a potential target in human schwannomas. Exp Neurol 218:137–144.

Flaiz C, Utermark T, Parkinson DB, Poetsch A, Hanemann CO. 2008. Impaired intercellular adhesion and immature adherens junctions in merlin-deficient human primary schwannoma cells. GLIA 56:506–515.

Georgakis GV, Li Y, Rassidakis GZ, Medeiros LJ, Younes A. 2006. The HSP90 inhibitor 17-AAG synergizes with doxorubicin and U0126 in anaplastic large cell lymphoma irrespective of ALK expression. Exp Hematol 34:1670–1679.

Girnita A, Girnita L, del Prete F, Bartolazzi A, Larsson O, Axelson M. 2004. Cyclolignans as inhibitors of the insulin-like growth factor-1 receptor and malignant cell growth. Cancer Res 64:236–242.

Gong Y, Yao E, Shen R, Goel A, Arcila M, Teruya-Feldstein J, Zakowski MF, Frankel S, Peifer M, Thomas RK, Ladanyi M, Pao W. 2009. High expression levels of total IGF-1R and sensitivity of NSCLC cells in vitro to an anti-IGF-1R antibody (R1507). PLoS One 4:e7273.

Hanemann CO, Bartelt-Kirbach B, Diebold R, Kampchen K, Langmesser S, Utermark T. 2006. Differential gene expression between human schwannoma and control Schwann cells. Neuropathol Appl Neurobiol 32:605–614.

Hanemann CO, Gabreels-Festen AA, Stoll G, Mueller HW. 1997. Schwann cell differentiation in Charcot–Marie–Tooth disease type 1A (CMT1A): Normal number of myelinating Schwann cells in young CMT1A patients and neural cell adhesion molecule expression in onion bulbs. Acta Neuropathol 94:310–315.

Harding TC, Xue L, Bienemann A, Haywood D, Dickens M, Tolkovsky AM, Uney JB. 2001. Inhibition of JNK by overexpression of the JNL binding domain of JIP-1 prevents apoptosis in sympathetic neurons. J Biol Chem 276:4531–4534.

Hebert E. 2006. Mannose-6-phosphate/insulin-like growth factor II receptor expression and tumor development. Biosci Rep 26:7–17.

Hiromura M, Okada F, Obata T, Auguin D, Shibata T, Roumestand C, Noguchi M. 2004. Inhibition of Akt kinase activity by a peptide span-

ning the betaA strand of the proto-oncogene TCL1. J Biol Chem 279:53407–53418.
Kaempchen K, Mielke K, Utermark T, Langmesser S, Hanemann CO. 2003. Upregulation of the Rac1/JNK signaling pathway in primary human schwannoma cells. Hum Mol Genet 12:1211–1221.
Kim RJ, Kim SR, Roh KJ, Park SB, Park JR, Kang KS, Kong G, Tang B, Yang YA, Kohn EA, Wakefield LM, Nam JS. 2010. Ras activation contributes to the maintenance and expansion of Sca-1pos cells in a mouse model of breast cancer. Cancer Lett 287:172–181.
Kolb EA, Kamara D, Zhang W, Lin J, Hingorani P, Baker L, Houghton P, Gorlick R. 2010. R1507, a fully human monoclonal antibody targeting IGF-1R, is effective alone and in combination with rapamycin in inhibiting growth of osteosarcoma xenografts. Pediatr Blood Cancer 55:67–75.
Korinthenberg R, Sauer M, Ketelsen UP, Hanemann CO, Stoll G, Graf M, Baborie A, Volk B, Wirth B, Rudnik-Schoeneborn S, Baborie A, Volk B, Wirth B, Rudnik-Schöneborn S, Zerres K. 1997. Congenital axonal neuropathy caused by deletions in the spinal muscular atrophy region. Ann Neurol 42:364–368.
Kurzrock R, Patnaik A, Aisner J, Warren T, Leong S, Benjamin R, Eckhardt SG, Eid JE, Greig G, Habben K, Eid JE, Greig G, Habben K, McCarthy CD, Gore L. 2010. A phase I study of weekly R1507, a human monoclonal antibody insulin-like growth factor-I receptor antagonist, in patients with advanced solid tumors. Clin Cancer Res 16:2458–2465.
Lallemand D, Manent J, Couvelard A, Watilliaux A, Siena M, Chareyre F, Lampin A, Niwa-Kawakita M, Kalamarides M, Giovannini M. 2009. Merlin regulates transmembrane receptor accumulation and signaling at the plasma membrane in primary mouse Schwann cells and in human schwannomas. Oncogene 28:854–865.
Lee KH, Joung HA, Ahn JH, Kim KO, Oh IS, Shin YB, Kim MG, Kim DM. 2007. Real-time monitoring of cell-free protein synthesis on a surface plasmon resonance chip. Anal Biochem 366:170–174.
Lee TX, Packer MD, Huang J, Akhmametyeva EM, Kulp SK, Chen CS, Giovannini M, Jacob A, Welling DB, Chang LS. 2009. Growth inhibitory and anti-tumour activities of OSU-03012, a novel PDK-1 inhibitor, on vestibular schwannoma and malignant schwannoma cells. Eur J Cancer 45:1709–1720.
Lerner EC, Qian Y, Blaskovich MA, Fossum RD, Vogt A, Sun J, Cox AD, Der CJ, Hamilton AD, Sebti SM. 1995. Ras CAAX peptidomimetic FTI-277 selectively blocks oncogenic Ras signaling by inducing cytoplasmic accumulation of inactive Ras–Raf complexes. J Biol Chem 270:26802–26806.
Li W, You L, Cooper J, Schiavon G, Pepe-Caprio A, Zhou L, Ishii R, Giovannini M, Hanemann CO, Long SB, Hanemann CO, Long SB, Erdjument-Bromage H, Zhou P, Tempst P, Giancotti FG. 2010. Merlin/NF2 suppresses tumorigenesis by inhibiting the E3 ubiquitin ligase CRL4(DCAF1) in the nucleus. Cell 140:477–490.
McClatchey AI, Fehon RG. 2009. Merlin and the ERM proteins--regulators of receptor distribution and signaling at the cell cortex. Trends Cell Biol 19:198–206.
Meier C, Parmantier E, Brennan A, Mirsky R, Jessen KR. 1999. Developing Schwann cells acquire the ability to survive without axons by establishing an autocrine circuit involving insulin-like growth factor, neurotrophin-3, and platelet-derived growth factor-BB. J Neurosci 19:3847–3859.
Momcilovic M, Miljkovic Z, Popadic D, Markovic M, Savic E, Ramic Z, Miljkovic D, Mostarica-Stojkovic M. 2008. Methylprednisolone inhibits interleukin-17 and interferon-gamma expression by both naive and primed T cells. BMC Immunol 9:47.
Morgan L, Jessen KR, Mirsky R. 1994. Negative regulation of the P0 gene in Schwann cells: Suppression of P0 mRNA and protein induction in cultured Schwann cells by FGF2 and TGF beta 1, TGF beta 2 and TGF beta 3. Development 120:1399–1409.
Ogata T, Iijima S, Hoshikawa S, Miura T, Yamamoto S, Oda H, Nakamura K, Tanaka S. 2004. Opposing extracellular signal-regulated kinase and Akt pathways control Schwann cell myelination. J Neurosci 24:6724–6732.
Ohshima-Hosoyama S, Hosoyama T, Nelon LD, Keller C. 2010. IGF-1 receptor inhibition by picropodophyllin in medulloblastoma. Biochem Biophys Res Commun 399:727–732.
Parkinson DB, Bhaskaran A, Droggiti A, Dickinson S, D'Antonio M, Mirsky R, Jessen KR. 2004. Krox-20 inhibits Jun-NH2-terminal kinase/c-Jun to control Schwann cell proliferation and death. J Cell Biol 164:385–394.
Rexhepaj R, Rotte A, Pasham V, Gu S, Kempe DS, Lang F. 2010. PI3 kinase and PDK1 in the regulation of the electrogenic intestinal dipeptide transport. Cell Physiol Biochem 25:715–722.
Rosenbaum C, Kluwe L, Mautner VF, Friedrich RE, Mueller HW, Hanemann CO. 1998. Isolation and characterization of Schwann cells from neurofibromatosis type 2 patients. Neurobiol Dis 5:55–64.
Rouleau GA, Merel P, Lutchman M, Sanson M, Zucman J, Marineau C, Hoang-Xuan K, Demczuk S, Desmaze C, Plougastel B. 1993. Alteration in a new gene encoding a putative membrane-organizing protein causes neuro-fibromatosis type 2 (see comments). Nature 363:515–521.
Sakai H, Nishimura A, Watanabe Y, Nishizawa Y, Hashimoto Y, Chiba Y, Misawa M. 2010. Involvement of Src family kinase activation in angiotensin II-induced hyperresponsiveness of rat bronchial smooth muscle. Peptides 31:2216–2221.
Schedlich LJ, Nilsen T, John AP, Jans DA, Baxter RC. 2003. Phosphorylation of insulin-like growth factor binding protein-3 by deoxyribonucleic acid-dependent protein kinase reduces ligand binding and enhances nuclear accumulation. Endocrinology 144:1984–1993.
Schumacher M, Jung-Testas I, Robel P, Baulieu EE. 1993. Insulin-like growth factor I: A mitogen for rat Schwann cells in the presence of elevated levels of cyclic AMP. Glia 8:232–240.
Sehat B, Tofigh A, Lin Y, Trocme E, Liljedahl U, Lagergren J, Larsson O. 2010. SUMOylation mediates the nuclear translocation and signaling of the IGF-1 receptor. Sci Signal 3:ra10.
Shi YQ, Blattmann H, Crompton NE. 2001. Wortmannin selectively enhances radiation-induced apoptosis in proliferative but not quiescent cells. Int J Radiat Oncol Biol Phys 49:421–425.
Toullec D, Pianetti P, Coste H, Bellevergue P, Grand-Perret T, Ajakane M, Baudet V, Boissin P, Boursier E, Loriolle F. 1991. The bisindolylmaleimide GF 109203X is a potent and selective inhibitor of protein kinase C. J Biol Chem 266:15771–15781.
Utermark T, Alekov A, Lerche H, Abramowski V, Giovannini M, Hanemann CO. 2003a. Quinidine impairs proliferation of neurofibromatosis type 2-deficient human malignant mesothelioma cells. Cancer 97:1955–1962.
Utermark T, Kaempchen K, Antoniadis G, Hanemann CO. 2005. Reduced apoptosis rates in human schwannomas. Brain Pathol 15:17–22.
Utermark T, Kaempchen K, Hanemann CO. 2003b. Pathological adhesion of primary human schwannoma cells is dependent on altered expression of integrins. Brain Pathol 13:352–363.
Walsh PT, Smith LM, O'Connor R. 2002. Insulin-like growth factor-1 activates Akt and Jun N-terminal kinases (JNKs) in promoting the survival of T lymphocytes. Immunology 107:461–471.
Wymann MP, Zvelebil M, Laffargue M. 2003. Phosphoinositide 3-kinase signalling—Which way to target? Trends Pharmacol Sci 24:366–376.
Xiao GH, Gallagher R, Shetler J, Skele K, Altomare DA, Pestell RG, Jhanwar S, Testa JR. 2005. The NF2 tumor suppressor gene product, merlin, inhibits cell proliferation and cell cycle progression by repressing cyclin D1 expression. Mol Cell Biol 25:2384–2394.
Zhang M, Zhou Q, Liang QQ, Li CG, Holz JD, Tang D, Sheu TJ, Li TF, Shi Q, Wang YJ. 2009. IGF-1 regulation of type II collagen and MMP-13 expression in rat endplate chondrocytes via distinct signaling pathways. Osteoarthritis Cartilage 17:100–106.
Zhao J, Guan JL. 2009. Signal transduction by focal adhesion kinase in cancer. Cancer Metastasis Rev 28:35–49.